Formation of NO and N_2O during Raw and Demineralized Biomass Char Combustion

Ulusoy, Burak; Lin, Weigang; Karlström, Oskar; Li, Songgeng; Song, Wenli; Glarborg, Peter; Dam-Johansen, Kim; Wu, Hao

Published in:
Energy and Fuels

Link to article, DOI:
10.1021/acs.energyfuels.9b00622

Publication date:
2019

Document Version
Peer reviewed version

Formation of NO and N_2O during raw and demineralized biomass char combustion

Burak Ulusoy [1,2,3], *Weigang Lin* [1,3], *Oskar Karlström* [4], *Songgeng Li* [3,5], *Wenli Song* [3,5], *Peter Glarborg* [1], *Kim Dam-Johansen* [1], *Hao Wu* [1*]

1: Department of Chemical and Biochemical Engineering, Technical University of Denmark, Søltofts Plads 229, 2800 Kgs. Lyngby, Denmark

2: Sino-Danish Centre for Education and Research, Beijing, China

3: Sino-Danish College, University of Chinese Academy of Sciences, Beijing 100049, China

4: Johan Gadolin Process Chemistry Centre, Åbo Akademi University, Finland

5: State Key Laboratory of Multiphase Complex Systems, Institute of Process Engineering, Chinese Academy of Sciences, Beijing 100190, China

Keywords: Biomass, char, nitrogen oxides, NO, N_2O, char nitrogen conversion, NO reduction

***Corresponding author e-mail id:** haw@kt.dtu.dk

Most recent modification date: 29-Apr-19

Abstract: The formation of nitrogen oxides (NO and N_2O) during raw and demineralized biomass char combustion and the reduction of NO over biomass char were investigated. The biomass fuels were pine wood, straw, waste wood, bran, dried distillers grains with solubles (DDGS), and sunflower seed. Fixed bed combustion experiments were performed at 800°C in 10vol% O_2, while NO reduction experiments were conducted at temperatures from 800 to 900°C and NO inlet concentrations from 400 to 1500 ppmv. The chars were characterized by means of ICP-OES, BET, SEM-EDX, and XPS. The conversion of char-N to NO decreased with an increase in the initial char-N content, partly explained by the increased inherent conversion of char-N to N_2O. The reduction of NO over char exhibited no correlation to the surface functionalities and content of nitrogen and oxygen at the investigated conditions. The NO reduction reactivity was strongly dominated by the content and association of ash forming elements in the chars. The NO reduction reactivity of pine wood, waste wood, and straw chars correlated reasonably well with the (K+Ca)/C molar ratio, while the chars with a high phosphorous content, i.e., bran, DDGS, and sunflower seed chars, differed by showing a significantly lower reactivity. The inhibition effect of phosphorous on NO reduction reactivity was likely caused by the formation of less catalytically active potassium species (such as KPO_3) in biomass char.

Introduction

Minimizing nitrogen oxides (NO_X) emissions from industrial solid fuel combustion is important due to the harmful environmental impact and strict emission regulations. In fluidized bed combustion (FBC), NO_X primarily stems from the fuel bound nitrogen through volatile and char oxidation. While the gaseous nitrogen chemistry is fairly well established,[1,2] the conversion of char-N to NO is less understood, especially in the case of high-nitrogen biomass fuels. During char combustion, NO is simultaneously formed from and reduced by char. The final emission of NO_X is determined by the competing NO_X formation and reduction reactions.[3]

The products of char nitrogen combustion include primarily NO, N_2O, and N_2.[4] During fixed bed coal char combustion at single particle conditions, the conversion of char-N to NO ranged from 75-100%.[4,5] Similar experiments employing biomass chars yielded char-N to NO conversions in a range of 25-75%, implying a significant reduction of NO during biomass char combustion.[6] The fractional conversion of char-N depends on the operating conditions (such as temperature and gas composition) and the fuel properties.[4]

The proposed mechanism for the formation and reduction of NO during char combustion in an O_2/N_2 system is summarized in R1-R2 and R3-R9, repectively.[7–11] Here, (-CX) denotes a carbon surface complex of either nitrogen or oxygen, while (-C) is a free carbon active site and M is a catalytically active ash forming element. The dissociative chemisorption of NO occurs in R3 and R7 followed by reduction through R4 and R5, and active site regeneration by R8 and R9. Additionally, the presence of CO has been reported to enhance the reduction reaction,[12] presumably by reaction with NO catalyzed by char, demonstrated by the non-elementary R6. Ultimately, the (-CO) is released to the gas phase as CO or CO_2, and a free active site is formed. Several reviews dealing with the reduction reaction between NO and coal char have been

reported.[3,4,13–15] Compared to coal, biomass chars generally exhibit a higher reactivity towards NO reduction.[8,12,16] This has been attributed the higher potassium content and larger surface area of biomass chars. Besides these, other factors such as increased amounts of sodium[17], magnesium[18], calcium, and iron[19], and more effective porosity[20] have been shown to enhance the NO reduction reactivity.

$$O_2 + (\text{-C}) + (\text{-CN}) \rightarrow (\text{-CO}) + (\text{-CNO}) \quad \text{R1}$$

$$(\text{-CNO}) \rightarrow NO + (\text{-C}) \quad \text{R2}$$

$$NO + 2\,(\text{-C}) \rightarrow (\text{-CO}) + (\text{-CN}) \quad \text{R3}$$

$$2\,(\text{-CN}) \rightarrow N_2 + 2\,(\text{-C}) \quad \text{R4}$$

$$(\text{-CN}) + NO \rightarrow N_2 + (\text{-CO}) \quad \text{R5}$$

$$2\,NO + 2\,CO \rightarrow N_2 + 2\,CO_2 \quad \text{(over char)} \quad \text{R6}$$

$$(\text{-M}_x\text{O}_y) + (\text{-C}) + NO \rightarrow (\text{-M}_x\text{O}_{y+1}) + (\text{-CN}) \quad \text{R7}$$

$$(\text{-M}_x\text{O}_{y+1}) + (\text{-C}) \rightarrow (\text{-M}_x\text{O}_y) + (\text{-CO}) \quad \text{R8}$$

$$(\text{-CO}) \rightarrow CO + (\text{-C}) \quad \text{R9}$$

Studies have shown that the conversion of char-N to NO decreased with an increase in char-N content and external NO concentration.[8,21,22] This effect was more pronounced with demineralized biomass, wherein the influence of the inorganics was minimized.[8] These results indicate that the formation and reduction of NO are related to the initial char-N content and gas phase NO concentration. The reaction rate between char and NO was suggested to be proportionally correlated to the instantaneous NO and C(N) concentrations.[7] R3-R9 are indicative that higher contents of char-N and ash forming elements would lead to higher NO reduction rates. Consequently, the reactivity of high-nitrogen chars towards NO could conceivably be enhanced by the initial char-N content. In addition, although the influence of the ash forming elements on

the char NO reactivity has been well documented[8,12], the importance of their association in the raw biomass is still unclear.

To obtain an improved understanding of the declining tendency in char-N conversion to NO with an increase in char-N content, a thorough study of the NO formation and reduction during raw and demineralized biomass char combustion was conducted in a fixed bed reactor at conditions relevant to fluidized bed combustion. The product distribution from char-N oxidation was characterized and its dependency on the chemical composition of the chars was investigated. The NO reduction reactivity of the chars was examined at different temperatures and NO inlet concentrations. The results were interpreted based on analyses of the surface area, char-N content, nitrogen and oxygen surface functionality, and ash forming element content and association in biomass chars.

Experimental Section

Fuels and their demineralization

Six types of biomass, pine wood, straw, waste wood, bran, dried distillers grains with solubles (DDGS), and sunflower seed, were employed in the experiments. Table 1 shows the composition of selected elements in the raw fuels. The complete compositions are given in the supplemental material (Table S1). The nitrogen contents ranged from 0.2 to 6.14 wt%, thereby covering a wide range of nitrogen contents in biomass fuels.

Table 1. Chemical composition of the six biomass.

	[wt% d.b]						[mg/kg d.b.]					
Fuel	**C**	**H**	**N**	**O**	**S**	**Ash**	**K**	**P**	**Mg**	**Ca**	**Fe**	**Na**
Pine wood	51.5	6.20	<0.20	41.9	0.007	0.2	480	52	140	950	26	95
Straw	46.9	6.00	0.56	42.2	0.120	4.2	14,000	910	960	2,300	41	230
Waste wood	49.0	6.13	1.33	41.8	0.037	1.7	703	93	443	3,200	363	326
Bran	45.0	6.30	2.65	40.6	0.19	5.3	13,000	11,000	3,800	920	210	50
Sunfl. seed	40.5	5.73	6.14	33.4	0.23	14	18,416	12,810	6,724	7,328	1,730	410
DDGS	43.7	6.55	5.13	37.8	0.41	6.4	11,723	10,204	3,442	1,105	91	3,255

The biomass samples were demineralized (DM) following the work of Aho et al.[23] Biomass was initially ground and sieved to a size range of 212-1000 µm and subsequently suspended in 500 mL of HNO_3 (Sigma Aldrich, CAS number: 7697-37-2) solution at pH 2 and heated to 60°C. The leaching was continued for one hour at 60°C under stirring at 750 rpm. After one hour, the solids were collected by filtration and the leaching process repeated. Then, the biomass was filtered with 250 mL demineralized water until the permeate pH was above 6.0. The obtained demineralized biomass was dried at 105°C for one day.

A chemical fractionation method was used to separate the different groups of ash forming elements in straw.[24–27] To eliminate the influence of water-soluble materials such as alkali sulfates, carbonates, chlorides, and to a lesser extent organically bound metals, 30-35 g of straw was washed in 500 mL deionized water at room temperature under stirring at 750 rpm for 24 h. Subsequently, the liquid was removed by filtration, and the extraction process repeated. After the second leaching, the suspended solids were washed several times with 250 mL deionized water until the permeate pH was above 6.0. Following this, half of the water washed (WW) straw was dried at 105°C for one day, while the other half was suspended in 150 mL 1 M ammonium acetate (Fluka Chemica, CAS number: 631-61-8) to remove ion-exchangeable cations in the form of organically bound metals. The ammonium acetate treatment was continued for one day under stirring at 750 rpm, after which the organic washed (OW) straw was washed using 100 mL, 1 M ammonium acetate for the first wash and 250 mL deionized water for the subsequent washes until the permeate pH was above 6.0. The filtered solids were dried at 105°C for one day.

Char preparation

Chars from raw and DM biomass were prepared in a horizontal oven at 800°C using a N_2 flow of 2.5 NL/min. The pyrolysis temperature was monitored through a thermocouple placed in the middle of the oven. Upon reaching the desired temperature, approximately 10 g of biomass was quickly pushed into the reactor. The pyrolysis was continued for 10 minutes, after which the sample was rapidly withdrawn to a water cooled section to ensure prompt cooling. The char samples were withdrawn from the reactor below a temperature of approximately 150°C. The char yield was determined from the biomass and char mass.

Experimental setup

Figure 1 illustrates the quartz fixed bed reactor used for char combustion and NO reduction experiments.[10] The temperature in the bed was kept uniform by three independent heating elements and monitored by a thermocouple located 0.5 cm below the porous plate. Upon reaching the desired conditions, a solid feeding device enabled the introduction of a char-sand sample. In all experiments, 1.75 g quartz sand with a size of 250-355 μm, pre-treated at 800ºC, was added together with the char to facilitate sample admission and ensure a constant bed height. Blank tests confirmed that the sand itself had no reactivity towards NO reduction. NO reduction experiments were conducted at three temperatures (800, 850, 900ºC) and NO inlet concentrations (400, 800, 1500 ppmv) using 20-50 mg char with a size of 125-180 μm to diminish mass transport resistances. The influence of external and internal mass transfer limitations during NO reduction over char were assessed based on the Maer and Weisz-Prater criteria, respectively.[28] The results, summarized in the supplemental information (Table S2) for the most reactive biomass, straw, showed that the influence of mass transfer limitations was negligible at the highest applied temperature. Following a reduction experiment, 10% O_2 was introduced the reactor to burn the NO treated char. In addition, separate combustion experiments using 20 mg, 125-180 μm char were carried out at 800ºC in 10% O_2. The temperature in the sample bed was assumed constant during combustion in consequence of the low percentage of char in the bed and the high heat capacity of sand. In all experiments, the total volumetric flow rate was 1 NL/min with the balance gas being N_2. The CO, CO_2, O_2, and NO concentrations in the dry flue gas were continuously monitored by a series of on-line gas analyzers (NGA2000, Fischer-Rosemount). Moreover, a Fourier Transform Infrared Spectrometer (FTIR) (Multigas 2030 FTIR, MKS instruments) was employed in selected experiments to determine the distribution of nitrogen products during combustion.

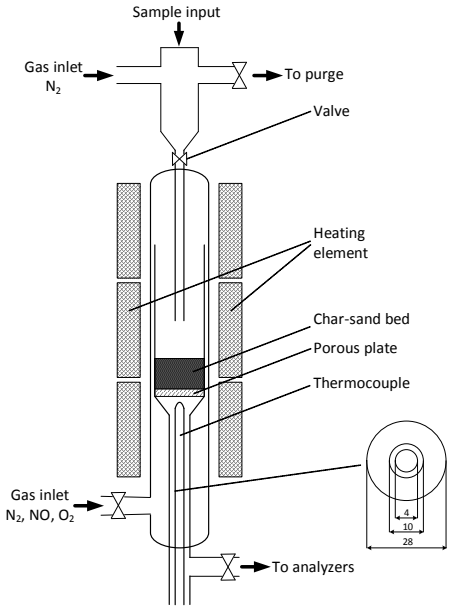

Figure 1. Schematic illustration of the fixed bed reactor. Adopted from Ulusoy et al.[10]

The reactivities of solid fuel chars towards NO are commonly evaluated from globalized first[29–32] or fractional[12,33,34] order rate expressions, where the rate constant is most frequently based on the instantaneous mass of carbon in the char. To compare the reactivities between chars, the first order rate constant of the NO-char reaction was determined under the assumption of plug flow, shown in Eq. 1.

$$-\ln\left(1-X_{NO}\right)=\frac{k_{NO}\cdot W}{v_g} \qquad \text{Eq. 1}$$

Here, X_{NO} (-) is the instantaneous conversion of NO, W (kg C) the instantaneous char carbon mass in the bed, v_g (m^3/s) the volumetric gas flowrate, and k_{NO} ($m^3\ s^{-1}\ kgC^{-1}$) the first order carbon mass based rate constant. The instantaneous carbon mass was determined from the CO and CO_2 measurements during the reduction section, while the total C-content from a mass balance of the entire experiment.

Characterization of chars

The specific Brunauer-Emmett-Teller (BET) surface area and the Barrett-Joyner-Halenda (BJH) mesoporosity of the chars were determined from N_2 adsorption at its boiling point (77 K) in the p/p_0 range of 0.01-0.99 using a Quantachrome iO2 equipment. Prior to measurements, the samples were vacuum degassed at 300°C for 5 h. Scanning electron microscopy and energy dispersive x-ray (SEM-EDX) analysis was performed on a selected number of chars. In the pre-treatment, the chars were coated with platinum, after which they were dried at 105°C for one day. X-ray photoelectron spectroscopy (XPS) was conducted on selected chars to analyze the content and functionalities of nitrogen and oxygen on the char surface. The C1s and N1s peaks were deconvolved using XPS PEAK 4.1 software by subtracting a Shirley type background and fitting Gaussian-Lorentzian mix functions. The nitrogen functionality was determined from 395-408 eV, in which five distinct nitrogen peaks, pyridinic N-6 (398.7±0.3), pyrrolic N-5 (400.3±0.3), quartenary N-Q (401.4±0.5), oxides N-X1 and N-X2 (402-405), were assigned.[35] The parameters used for the fitting were the peak width, position, and full-width-half-maximum (FWHM). The Gaussian-Lorentzian (G/L) mix, describing instrumental and metallic effects, was set at 0.7, i.e. 70% Gaussian and 30% Lorentzian for all nitrogen functionalities.

The chemical composition of the chars was analysed with a Thermo Scientific Flash 2000 Organic Elemental Analyser (Flash 2000) for the carbon, hydrogen, nitrogen, and sulphur content, while the inorganic contents were determined by inductively coupled plasma emission spectroscopy (ICP-OES).

Table 2 summarizes the chemical analyses of the chars, including selected ICP-OES results. The demineralized chars exhibited a lower ash content in comparison with the raw chars. Straw, bran, sunflower seed, and DDGS chars contained large amounts of potassium, which is presumably the most active catalytic element in the char-NO reaction. In comparison, the demineralized chars

were largely depleted of elements presumed to have a catalytic effect on the NO reduction, i.e. potassium, iron, calcium, sodium, and magnesium.

Table 2. Char elemental and proximate analyses of six raw and demineralized biomass.

	[wt% d.b.]							[mg/kg d.b.]					
Char	**C**	**H**	**N**	**O**	**S**	**Ash**	**Char yield**	**K**	**P**	**Mg**	**Ca**	**Fe**	**Na**
Pine wood	85.7	1.48	0.11	9.12	0.0	3.59	20.5	1,083	210	515	4,008	223	373
Straw	71.2	1.18	0.50	8.42	0.0	18.7	25.8	43,642	2,789	2,329	4,459	<3	740
Waste wood	70.0	1.17	1.06	18.4	0.0	9.36	20.8	1,977	355	3,505	32,002	4,426	1,152
Bran	59.9	1.30	2.90	9.90	0.0	26.0	26.5	69,610	49,429	18,304	3,629	676	<120
Sunfl. seed	57.0	1.10	3.59	11.2	0.0	27.1	29.4	55,749	29,190	17,100	18,101	2,446	550
DDGS	59.0	1.30	5.36	13.2	0.0	21.1	26.9	31,430	31,355	11,779	3,758	443	11,697
DM pine wood	87.5	1.56	0.11	10.7	0.0	0.11	15.8	<20	<60	<0.2	90	442	<120
DM straw	82.2	1.53	0.83	7.04	0.0	8.40	16.9	76	450	<0.2	212	77	<120
DM waste wood	74.8	1.23	0.84	16.5	0.0	6.59	17.4	245	194	1,606	8,845	1,483	<120
DM bran	76.9	1.49	3.52	7.69	0.0	10.4	25.7	129	13,702	32	96	1,047	<120
DM sunfl. seed	71.7	1.24	4.50	8.26	0.0	14.3	25.0	874	14,327	485	1,400	2,275	<120
DM DDGS	73.3	1.35	6.92	9.58	0.0	8.85	23.8	<20	8,402	<0.2	87	540	<120

Table 3 shows the physical properties of the chars. In general, the surface area and pore volume were noted to increase due to demineralization. The only exception to this was in the case of pine wood, where demineralized pine wood char showed a significantly lower surface area and pore volume, the reasoning of which is unknown. The large pore volume in some chars was primarily due to the formation of micropores in addition to mesopores during charring. A wide range of surface areas and pore volumes are covered by the investigated chars.

Table 3: BET surface area (SA), pore volume (V_p), and mean pore diameter ($d_{p,mean}$) of the chars.

Char	SA [m^2/g]	V_P [cm^3/g]	$d_{p,mean}$ [nm]
Pine wood	405	0.18	1.076/3.377
Straw	25	$2.4 \cdot 10^{-2}$	3.404
Waste wood	91	$5.8 \cdot 10^{-2}$	4.275
Bran	4.5	$6.1 \cdot 10^{-3}$	3.054
Sunfl. seed	1.2	$2.7 \cdot 10^{-3}$	3.855
DDGS	1.0	$1.2 \cdot 10^{-3}$	3.087
DM pine wood	4.5	$6.5 \cdot 10^{-3}$	3.059
DM straw	430	0.18	1.932/3.382
DM waste wood	415	0.18	1.178/3.383
DM bran	3.0	$3.1 \cdot 10^{-3}$	3.379
DM sunfl. seed	135	$6.8 \cdot 10^{-2}$	3.374
DM DDGS	4.6	$4.7 \cdot 10^{-3}$	3.440

173

Results

Conversion of char-N to NO

Figure 2 illustrates the conversion of char-N to NO during combustion of raw (a) and demineralized (b) chars in 10 % O_2, along with error bars depicting the deviations in the elemental analyses. The results indicate that the conversion of char-N to NO decreased with an increase in char-N content, in accordance with previous single particle combustion studies.[8,21] This trend was also observed for the demineralized chars at both investigated temperatures. At higher temperature, a slight increase in the conversion of char-N to NO was observed. Previous studies on coal chars showed that the effect of temperature was negligible when increased from 800 to 900°C,[36] while it could be more pronounced when changing from 850 to 1150°C.[5] According to the mechanism shown in R1-R9, the observed trends are conceivably related to the NO formation and/or reduction reactions. In the demineralized chars, i.e., with a diminished impact of inorganic elements, it could be expected that R4 and R5 occur more rapidly when high local concentrations (-CN) and NO are prominent. Alternatively, nitrogen-rich compounds could form a higher concentration of alternative combustion products such as N_2O, N_2, and NO_2. Lastly, the lower conversion to NO could be caused by the combustion atmosphere, e.g. simultaneous presence of high O_2 and CO concentrations, thereby increasing the importance of R6 and R9, respectively. In the following sections, the combustion product distribution and NO reduction reactivity of the chars were examined to provide insight into the decreasing conversion of char-N to NO.

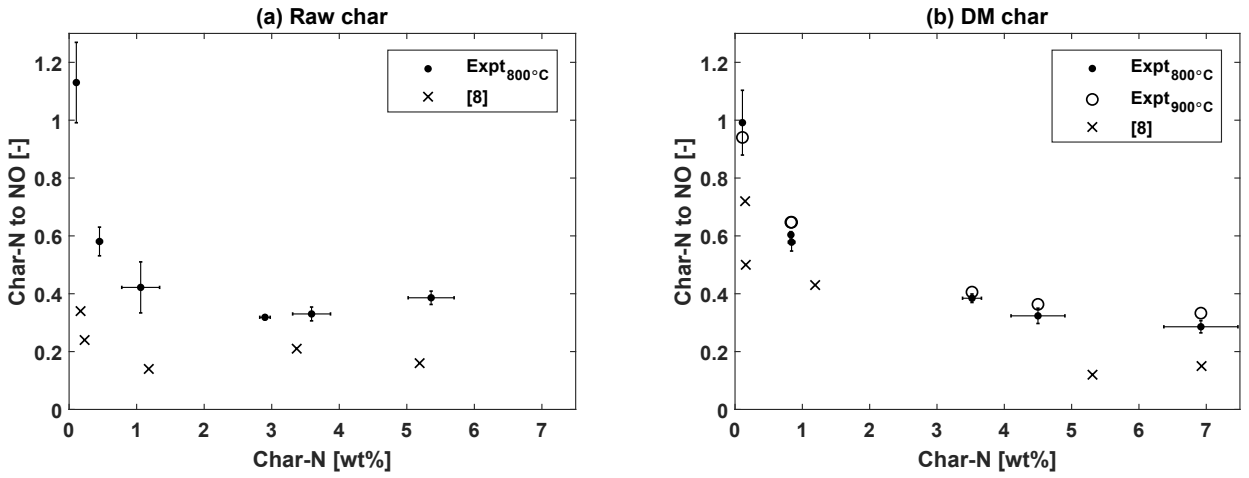

Figure 2. Conversion of char-N to NO during combustion of 20 mg raw (a) and DM (b) biomass char at 800°C in 10vol% O_2. The DM chars were additionally oxidized at 900°C. The measurement errors describe the deviations in the elemental analysis. For comparison, the data of Karlström et al.[8] at 900°C in 3vol% O_2 is shown.

Combustion product distribution of char-N

Figure 3 illustrates the FTIR determined nitrogen product distribution from raw and demineralized char combustion at 800°C in 10% O_2. The primary oxidation products were NO, N_2O, and a residual fraction, presumably consisting of N_2 and to lesser extent HCN, as negligible amounts of NH_3, HNCO, and NO_2 were detected. The HCN concentrations were not measured in the present study. In a combustion atmosphere without the addition of radical quenching compounds, the presence of HCN is expected to be low.[22,37,38] Consequently, the residual fraction is presumed to consist predominantly of N_2. The results show that a significant amount of N_2O was formed during biomass char combustion at 800°C, especially for the high-nitrogen chars. This is consistent with reported coal char combustion studies.[3,39] In addition, a slightly higher conversion to N_2O was observed for the demineralized chars, presumably caused by the promoting effect of ash forming elements such as potassium on the N_2O reduction over char.[40]

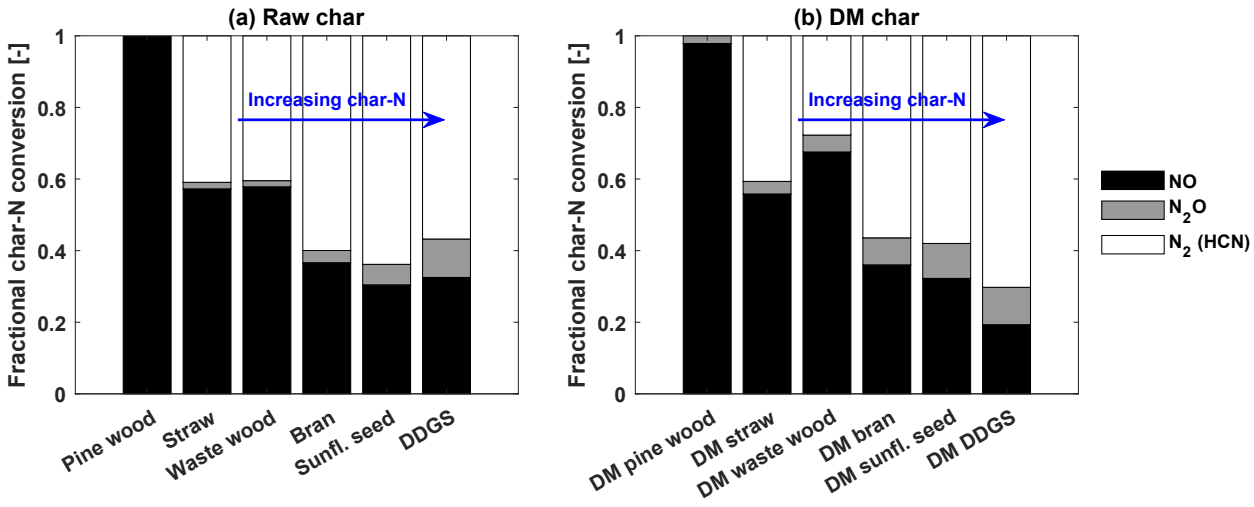

Figure 3. Distribution of nitrogen products from 20 mg char combustion at 800°C in 10vol% O_2.

Figure 4 illustrates the fractional conversion of char-N to NO and N_2O, and the ratio of N_2O to the total NO_X ($NO+N_2O$) during combustion of selected chars at varying char mass. By reducing the char mass, a smaller degree of reduction of the formed nitrogen oxidation products by secondary char particles is expected. The results show that high amounts of N_2O were formed during char combustion; in one case, as much as 25% of the char-N formed N_2O. The conversion of char-N to NO and N_2O generally increased with a decrease in char mass. In addition, the ratio of N_2O to the total NO_X was higher for the high-nitrogen DDGS chars and decreased with an increase in char mass, due to the faster decomposition of N_2O to N_2 over char (R10[39] and R11[15]) compared to NO.[41] As the reduction of reactive nitrogen combustion products by secondary char particles was small at low char mass, the results indicate that the inherent conversion of char-N to N_2O increased for a char size range of 125-180 µm. For different char sizes, the reduction within the parent char particle could be affected.[42] Two mechanisms have been proposed for the formation of N_2O during char combustion.[4] In the homogeneous mechanism, HCN or HNCO is released during char combustion, followed by reaction of the NCO radical with NO to form N_2O (R12-R13).[43] The heterogeneous mechanism involves the dissociative adsorption of O_2, followed by

reaction of the surface complex (-CNO) with a (-CN) site (R14) or NO molecule (R15). Negligible amounts of N_2O was detected by the reaction between NO and (-CN) without the presence of O_2;[12,44,45] this finding was verified by selected reduction experiments in this study. The relative importance R12-R13 and R14-R15 is yet unknown.[15] The larger amount of N_2O formed from combustion of high-nitrogen chars could possibly be explained by the high local concentrations of HCN and NO, or NO, (-CN), and (-CNO). Consequently, with an increase in char-N a higher fraction of char-N is inherently converted to N_2O, which is more readily reduced over char, thereby partly explaining the decrease in char-N to NO conversion with increasing char-N content. Besides affecting NO formation, a higher char-N content could conceivably enhance the NO reduction reactivity of the chars, which was further examined.

$$N_2O + (\text{-C}) \rightarrow N_2 + (\text{-CO}) \quad \text{R10}$$

$$N_2O + CO \rightarrow N_2 + CO_2 \quad \text{(over char)} \quad \text{R11}$$

$$HCN + O, OH \rightarrow NCO + H, H_2O \quad \text{R12}$$

$$NCO + NO \rightarrow N_2O + CO \quad \text{R13}$$

$$(\text{-CN}) + (\text{-CNO}) \rightarrow N_2O + 2\,(\text{-C}) \quad \text{R14}$$

$$NO + (\text{-CNO}) \rightarrow N_2O + (\text{-CO}) \quad \text{R15}$$

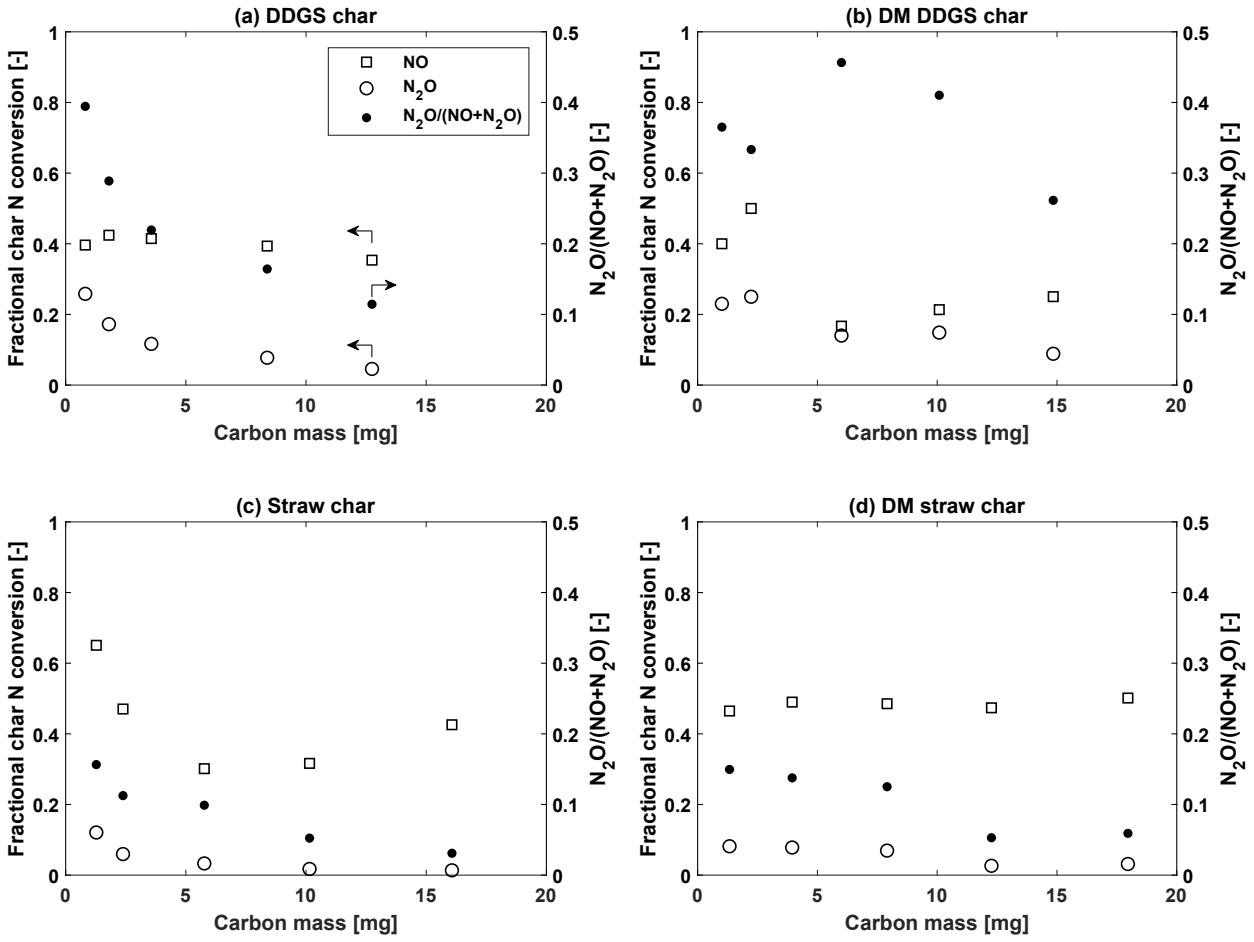

Figure 4. Conversion of char-N to NO and N_2O during combustion of DDGS (a), DM DDGS (b), straw (c), and DM straw (d) chars at varying mass at 800°C using 10vol% O_2.

Reduction of NO over raw and DM biomass chars

Figure 5 illustrates the conversion of 400 ppmv NO over the raw (a) and demineralized (b) biomass chars at 800°C. Of the raw biomass chars, the conversion of NO is high for straw, waste wood, and sunflower seed, while lower for bran, pine wood, and DDGS. The demineralized chars exhibited lower reduction in comparison to the raw chars and less discrepancy between different fuel chars. The maximum relative standard error between repetitions was determined to be 4%, demonstrated in the supplemental material (Figure S1). Based on the inherent nitrogen content of the chars in Table 2 and the conversion of char-N to NO in Figure 2, it was suspected that the

reduction reactivity of the demineralized chars in decreasing order would be DM DDGS, DM sunflower seed, DM bran, DM waste wood, DM straw, DM pine wood.

Figure 5c and d present the reactivity on a carbon mass basis of the chars at 800°C using 400 ppmv NO, calculated by Eq. 1. The difference in the raw chars was again more pronounced than that of the demineralized chars. For a majority of the chars, a high transient reactivity followed by a steady state is observed. This has previously been attributed to thermal deactivation, initial accumulation of NO on the char surface, or formation of thermally stable surface oxides.[4,33] In addition, mixing and delay of the gas stream downstream of the reactor contribute to the duration of this phase. The straw displayed the highest reactivity towards NO, presumably due to the large potassium content. Although the potassium in bran exceeded that of the straw, their reactivities differed significantly; this is further examined in the following sections. In addition, different transient behaviors of the chars was observed. In some cases, a distinct steady state was observed, e.g. bran and pine wood, while for other chars, e.g., from straw and waste wood, the reactivity significantly decreased with time. This in turn suggests that some chars are more prone to deactivation, possibly related to the transformation of catalytic inorganic species, which needs to be further studied. To correlate the observed trends in reactivity with the physiochemical properties of the chars, the transient reactivity was defined as the maximum rate constant. This reactivity was preferred over the steady state reactivity to minimize effects from long term, high temperature exposure. However, the conclusions for the transient reactivity also apply to the steady state reactivity. In addition, the influence of temperature and inlet NO concentration on the NO reduction reactivity of the chars was investigated. The results are generally in consensus with previous studies[4,12] and can be seen in the supplemental material (Figure S2 and S3). Although the reactivities were dependent on the NO inlet concentrations, the first order rate constant can be used

as a qualitative comparison of the char reactivity under similar NO concentration. For modelling purposes, other rate expressions such as fractional order, concentration averaged, or mechanistic models may be used to capture the effect of NO inlet concentration.

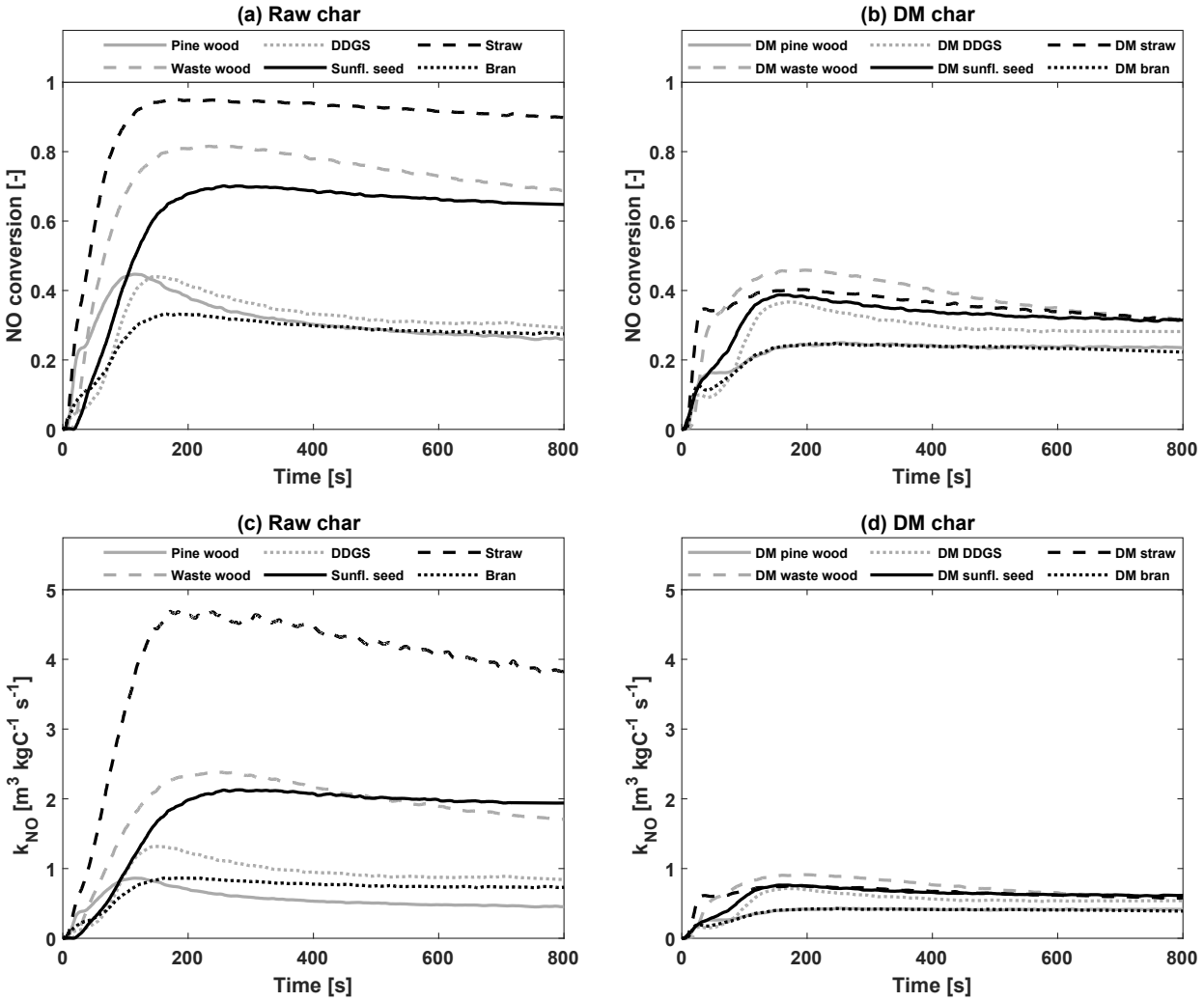

Figure 5. Conversion of NO over 50 mg raw (a) and DM (b) chars at 800°C using an NO inlet concentration of 400 ppmv NO. First order carbon mass based NO reduction rate constant (k_{NO}) against time for raw (c) and DM (d) chars at 800°C and 400 ppmv NO.

Influence of initial surface area and char-N content on NO reduction

Figure 6 demonstrates the reactivity as a function of BET surface area. A direct correlation between the reactivity and the initial BET surface area was not observed for any of the chars. As the surface areas of the chars were prone to change during reaction either by thermal annealing or pore opening, it may not be possible to rule out the effect of surface area on the NO reduction. Therefore, the relevant or active instantaneous surface area could provide a better basis for reactivity especially for the non-catalytic, demineralized chars.[46] A previous study suggested that the reactivity of chars towards NO correlated better with the specific surface area of the meso and macropores (>50 nm) determined by mercury intrusion.[20]

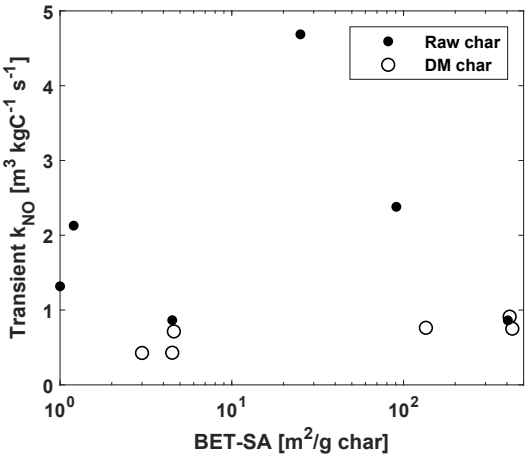

Figure 6. First order, transient NO reduction reactivity of DM and raw biomass chars against the BET surface area expressed in m^2/g. The rate constants were determined at 800°C using an NO inlet concentration of 400 ppmv.

Figure 7 demonstrates the reactivity of the demineralized and raw chars against the initial char-N content. No correlation was observed between the reactivity and the initial char-N content. In addition, no correlation was observed between the reactivity, and the product and ratio of char-N content and surface area, seen in the supplemental material (Figure S4). For the raw chars, the reasoning for this is most likely due to the stronger impact of catalytic elements. In comparison,

the demineralized chars showed a smaller discrepancy. The small differences in reactivity are presumably caused by distinct physical or chemical properties, all of which are prone to change during experimentation. Possible influential factors are the surface area, pore size distribution, and surface chemistry, the latter of which includes elemental population and functionality. Based on the results on the conversion of char-N to NO and the proposed reduction mechanism (R3-R9), it was hypothesized that a higher nitrogen content (-CN) would lead to a higher reduction reactivity of the demineralized chars through R4 and R5. The results here show no direct correlation between reactivity and initial char-N content. Although, the reactivities at 800°C are shown in Figures 6 and 7, the conclusions drawn here also apply at 900°C. Pevida et al.[47] reported a similar observation in their study, noting that the reactivities of model chars with and without (-CN) were quite similar. Hence, they concluded that the inherent nitrogen content had a small effect on the reduction reaction. The reduction reactivity of the accumulated (-CN) sites could be different relative to the inherent (-CN) sites, thereby explaining why no correlation to the inherent char-N content was observed. The buildup of (-CN) sites during NO reduction was demonstrated in this study by the combustion of NO treated and untreated chars at 900ºC. From these experiments, it was noted that the conversion of char-N to NO systematically increased with the concentration of NO during reduction experimentation, seen in Figure 8. The systematic increase in conversion was most likely caused by surface enrichment of (-CN) and (-CO) species during the NO reduction. Previous studies indicated a temperature dependent buildup of both (-CN) and (-CO) species during the NO-char reaction, during which the accumulation of (-CN) was greater than (-CO) at temperatures above 750°C.[7,48] An increase in (-CN) would increase the amount of NO formed from combustion, while (-CO) could have a promoting or inhibiting effect on the NO reduction,

depending on the bond strength. In the following section, the type and importance of the inherent surface nitrogen functionality is discussed.

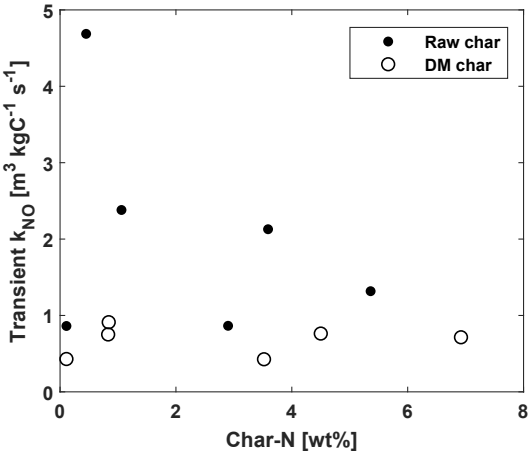

Figure 7. First order, transient NO reduction reactivity of DM and raw biomass chars against the initial nitrogen content. The rate constants were determined at 800°C using an NO inlet concentration of 400 ppmv.

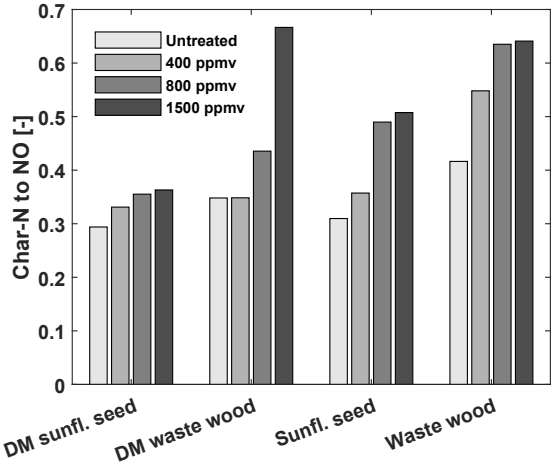

Figure 8. The conversion of char-N to NO (F_{NO}) from combustion of NO treated and untreated chars. $F_{NO} = \int_0^{t_{final}} NO dt / \left[\int_0^{t_{final}} CO + CO_2 dt \cdot \left(\frac{N}{C}\right)_{char}\right]$. Conditions of combustion: 900°C, 10vol% O_2. Conditions of NO treatment: 900°C, [400;1500] ppmv NO.

Influence of char nitrogen and oxygen functionality on NO reduction

Figure 9 displays the nitrogen functionality as determined by XPS. All chars contained large amounts of pyridinic (N6), pyrrolic (N5), and quartenary (NQ) nitrogen with differences in the relative distributions of these. In general, the relative abundance of N6 and NQ in chars increases with the severity of heat treatment, i.e., temperature and holding time, due to the thermal stabilities of these compounds.[35,49,50] The results here show a small discrepancy between the demineralized samples with the only exception being DM pine wood. Notably, the nitrogen content in this char was low, thereby raising question as to the usability of a deconvolution method for extracting functionality data, seen in supplemental material (Figure S5). Nonetheless, the results are shown here and treated critically in the correlation studies described below. In addition, the demineralization changed the nitrogen functionalities in the resulting char in the case of straw, while a lesser impact was observed for bran and sunflower seed. Previously, deashing of coals and their respective chars using stronger acids such as HCl and HF showed little or no change in the nitrogen functionality.[51] Thus, the change in nitrogen functionality for straw could therefore be due to the influence of ash forming elements on the pyrolysis, rather than the demineralization process itself.

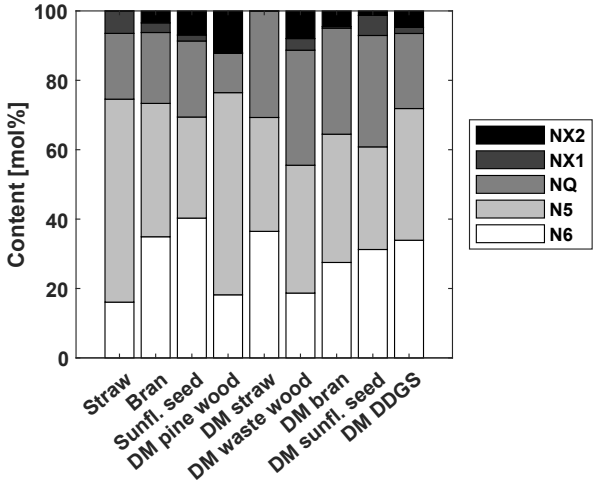

Figure 9. Surface nitrogen distribution as measured by XPS for selected raw and all demineralized chars.

Several studies have concluded that no correlation exists between the char-N functionality and NO emission in an oxidizing atmosphere.[15,52–55] This has primarily been attributed to the larger influence of other factors such as physical properties, catalytic effects, and NO reduction over char.[15] This study also implies a lack of correlations between the surface nitrogen/oxygen functionality and the measured NO formation and reduction, as shown in the supplemental material (Table S3-S4 and Figure S6-S7). Instead the char-N content was again determining for the fractional conversion to NO and N_2O during char combustion (Figure S8), further explained in the discussion section.

Influence of ash forming element content and association on NO reduction

It was previously stated that potassium, calcium, iron, magnesium, and sodium can catalyze the reduction of NO over char, most likely through reactions R7 and R8. Although, bran char contained considerably higher amounts of potassium and magnesium, and comparable amounts of calcium, iron, and sodium as straw char, the reactivity was significantly lower. A contributing factor to this could be the much larger phosphorous content in bran, which could capture the potassium and form presumably catalytically less active compounds, e.g., KPO_3.[56] A similar reasoning would describe the observed differences between the high-phosphorous sunflower seed and DDGS chars, and low-phosphorous straw char. To investigate this hypothesis, the surface composition of catalytic elements were examined using SEM-EDX measurements, illustrated in Figure 10 and Table 4. The straw char contained a rougher surface structure compared to the smoother bran char, thus explaining the smaller surface area of the latter. Both bran and straw char contained a large quantity of potassium on the surface, while bran char additionally showed a large phosphorous content. The ratio between these elements was approximately 1:1, thereby possibly indicating the presence of KPO_3 on the bran char surface, while the potassium in straw char was primarily present as organic-K, KCl, and to lesser extent K_2SO_4 and higher order minerals. As the magnitude of the surface areas of straw and bran char was comparable, the results here suggest that KPO_3 in bran char caused the lower NO reduction reactivity compared to straw char. However, further studies are necessary to clarify the influence of phosphorous on the NO reduction reactivity of chars.

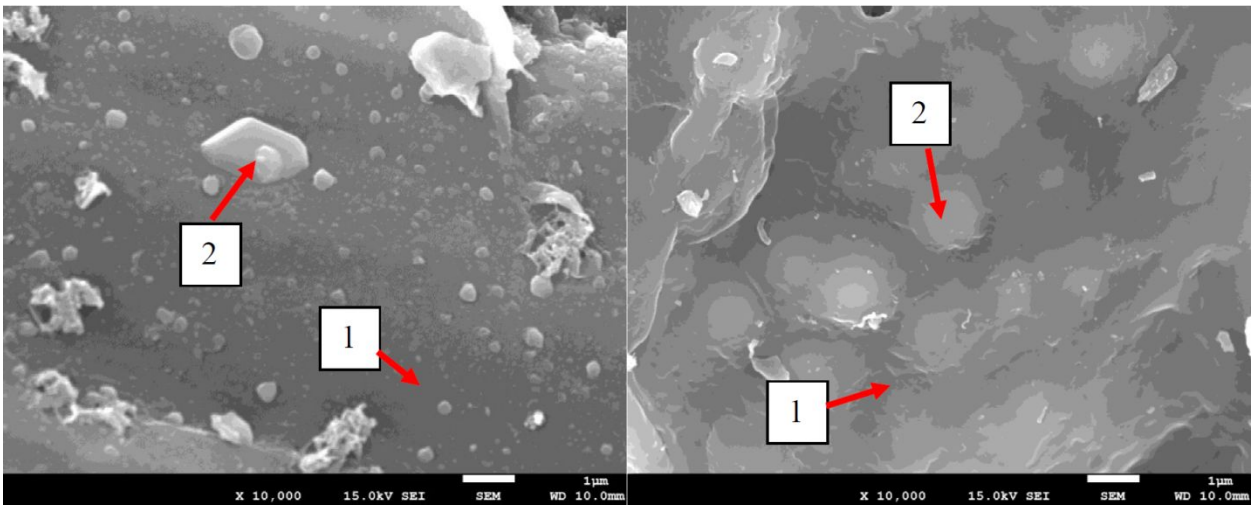

Figure 10. SEM-EDX measurements of straw (left) and bran (right)

Table 4. EDX results in connection to Figure 10.

[at%]

Char	K	P	Mg	Ca	Fe	Na	Cl	S
Straw 1	**6.7**	**1.7**	0.90	0.87	0.00	0.15	4.9	0.2
Straw 2	**3.5**	**0.1**	0.04	0.01	0.00	0.01	1.1	0.1
Bran 1	**7.0**	**7.1**	1.10	0.51	0.07	0.01	0.03	0.1
Bran 2	**4.6**	**5.8**	2.49	0.28	0.05	0.01	0.02	0.1

To determine the influence of ash forming element association in the raw straw, a sequential leaching method was employed. Table 5 summarizes selected chemical and physical properties of the raw and washed straw chars, along with the NO reduction reactivities. The results show that the ash content decreased with the severity of pre-treatment. Potassium, phosphorous, and sodium in the straw were predominately water soluble, while magnesium and to some extent calcium was organically bound. In addition, the surface area increased from raw to demineralized straw char, most likely due to the formation of micropores as a consequence of pre-treatment. The contribution

of water soluble, organically soluble, acid soluble, and insoluble ash forming elements to the total ash was 44.6%, 4.3%, 5.9%, and 45.2%, respectively. The presence of the ash forming elements on the surface was verified using SEM-EDX, which additionally showed little change in the morphology of the chars, seen in supplemental material (Figure S9 and S10). All char samples exhibited a rod shaped particle with a porous, tunnel-like structure. In addition, the reactivity decreased with the severity of pre-treatment. As the water soluble elements (secluded alkali or alkaline carbonates, chlorides, sulfates, and hydroxides) in straw had a large contribution to the total ash content, the influence of these on the reduction reactivity were higher. Moreover, the results show that the influence of ash forming elements dominates the reduction reactivity of the chars in comparison to other factors such as surface area and porosity.

Table 5. Chemical and physical properties of the sequentially leached chars. The reduction rate constant is the transient values from reduction experiments at 800°C using 400 ppmv NO.

	[wt% d.b.]						[mg/kg d.b.]						Physical properties			k_{NO}
Char	**C**	**H**	**N**	**O**	**S**	**Ash**	**K**	**P**	**Mg**	**Ca**	**Fe**	**Na**	**BET** [m^2/g]	**V_P** [cm^3/g]	**$d_{P,mean}$** [nm]	[m^3 kgC^{-1} s^{-1}]
Straw	71.2	1.18	0.50	8.42	0.0	18.7	43,642	2,789	2,329	4,459	<3	740	25	$2.4 \cdot 10^{-2}$	3.404	4.7
WW straw	78.9	1.36	0.41	8.93	0.0	10.4	3,047	235	2,175	5,714	92	<120	296	0.14	1.932/ 3.380	2.1
OW straw	71.7	1.29	0.50	16.9	0.0	9.60	<20	228	104	1,630	154	<120	421	0.18	1.932/ 3.389	0.97
DM straw	82.2	1.53	0.83	7.04	0.0	8.40	76	450	<0.2	212	77	<120	430	0.18	1.932/ 3.382	0.75

The NO reduction reactivity of all chars studied as a function of the molar (K+Ca)/C ratio is shown in Figure 11. In our previous study, the NO reduction reactivity of sewage sludge, RDF, and straw chars correlated well with the molar ratio (Fe+K+Ca)/C.[10] As the iron content in the

biomass chars was very low, Fe was neglected in this study. The results show that the reactivities of the low-phosphorous (pine wood, waste wood, and straw) chars correlated reasonably well with the (K+Ca)/C molar ratio at two temperatures. The reactivities of the raw high-phosphorous (bran, sunflower seed, and DDGS) chars were lower than the regression line, the reasoning of which has been discussed in previous paragraphs. Demineralized chars exhibited a lower discrepancy, thereby showing a lesser impact of phosphorous.

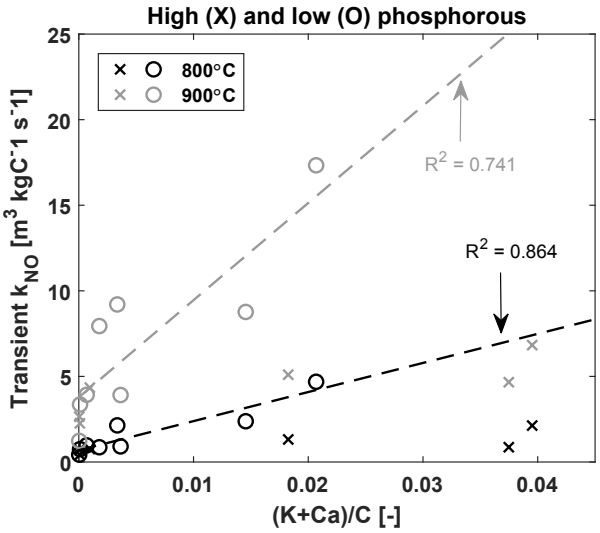

Figure 11. First order, transient NO reduction reactivity of all investigated chars at 800ºC and 900ºC using 400 ppmv NO against the molar ratio (K+Ca)/C. The regression lines were made solely on the low-phosphorous chars.

Discussion

Previous studies reported a decrease in the conversion of char-N to NO with an increase in char-N content, indicating that the reduction of the formed NO by char may be faster for high-nitrogen chars.[8,21] However, the conversion of char-N to NO did not correlate with the NO reduction reactivities of the chars as shown in Figure 12a. Combustion studies revealed a decreased formation of NO and an increased formation of N_2O with a higher char-N content at 800°C, seen in Figure 12b and c. During fixed bed combustion, the formed NO and N_2O could either react with the char from which it was produced or with other secondary char particles in the bed. To gain insight into the inherent conversion of char-N to NO and N_2O for a certain char particle size range, combustion experiments with varying char mass were conducted. The results revealed that the fractional conversion of char-N to N_2O increased with a decrease in char mass and an increase in char-N content. Hence, the investigated char particles inherently formed a large fraction of N_2O. This could to some extent explain the decreasing tendency of char-N to NO conversion with an increase in char-N, as the larger proportion of N_2O from combustion of high-nitrogen biomass chars is more readily reduced over char than NO. However, caution must be taken when interpolating these results obtained at 800°C to other temperatures, as the char-N conversion is temperature dependent.[3] The importance of N_2O has been shown to decrease with temperature, due to higher rates of competitive reactions and N_2O destruction.[4]

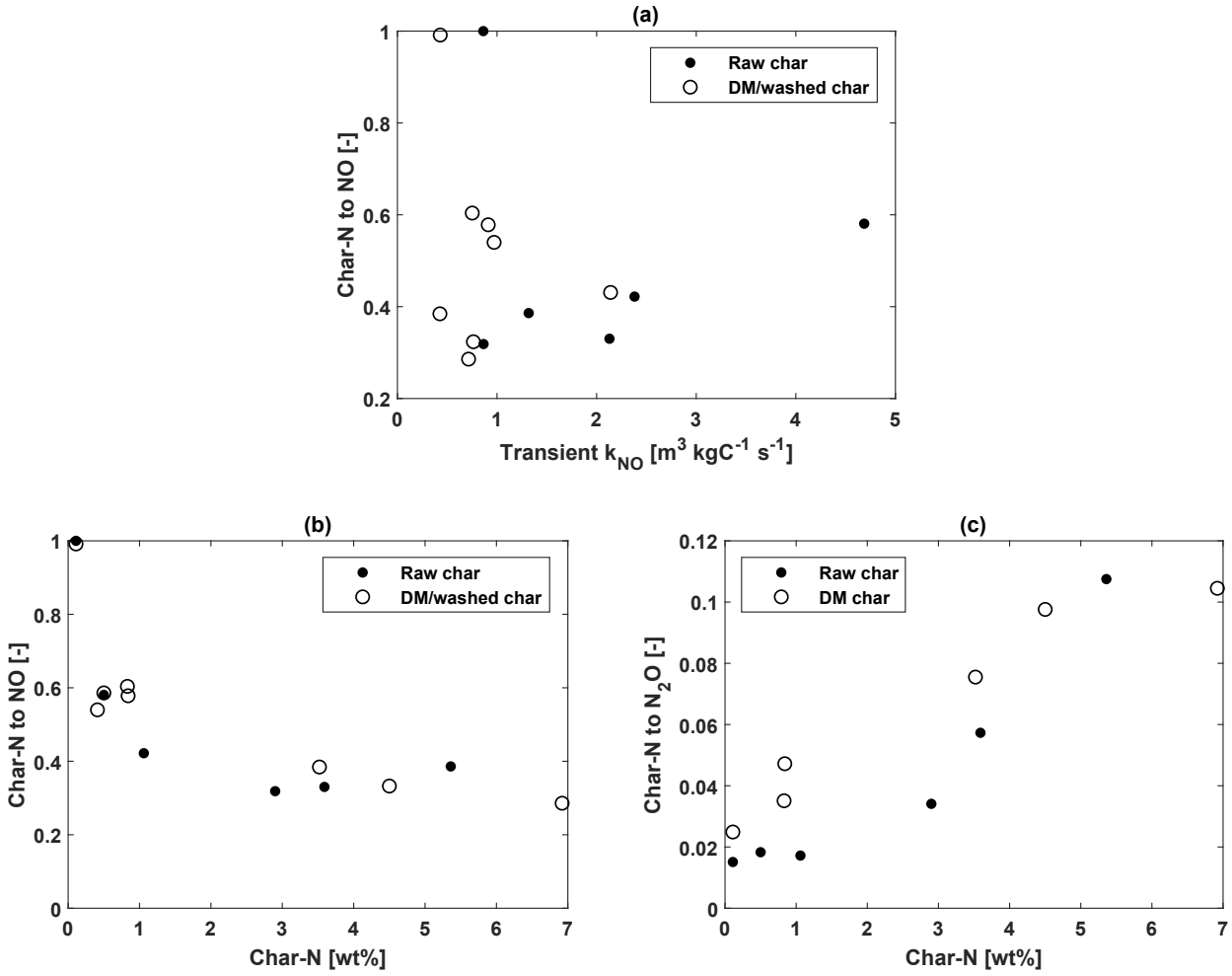

Figure 12. Char-N to NO conversion against the first order, transient NO reduction reactivity (a) and char-N content (b), and char-N to N_2O conversion against char-N content (c). The combustion properties were determined from 20 mg char combustion at 800°C in 10% O_2. The data for raw pine wood char has been corrected for fluctuations in the elemental analyses, i.e., set equal to 1.

While the formation of N_2O can partly explain the decreasing tendency of NO with the char-N content, additional factors could have a prominent effect. The most probable effects would be that of CO and O_2 on the NO reduction by R6 or R9, respectively. While the influence of CO on NO reduction in the inert NO reduction experiments was negligible due to the relatively low concentration, the contribution of this in a combustion atmosphere cannot be omitted. Effluent CO

concentrations were around 4000 ppmv and likely much higher near the char particle surface. The local concentrations of NO in high-nitrogen chars could likewise be high, thereby increasing the relative importance of R6. However, additional investigations are necessary to clarify the influence of R6 on the overall reduction of NO from combustion. In the case of O_2, NO reduction has generally been reported to be enhanced in the presence of O_2 either by oxidative active site generation (R9) or activation of (-CN).[57] Lastly, changes in surface properties and catalytic components with char conversion could have an important influence on the reactivities of the chars, which needs further study.

Conclusions

The conversion of char-N to NO during biomass char combustion decreased with an increase in the initial char-N content. As this trend did not correlate with the NO reduction reactivity of the chars, an important contributing factor may be the increased formation of N_2O with an increase in char-N content.

For NO reduction over biomass char, the reactivity was largely dominated by the association and content of ash forming minerals. The reactivities of chars containing a low content of phosphorous (pine wood, waste wood, and straw) correlated reasonably well with the (K+Ca)/C molar ratio. In comparison, the high-phosphorous (bran, DDGS, and sunflower seed) chars exhibited a lower NO reduction reactivity. A plausible explanation is that the potassium in chars with a high phosphorous content was bound in a catalytically less active form such as KPO_3. Other physical (initial surface area and porosity) and chemical (initial char-N content, and nitrogen and oxygen surface functionality and content) properties did not correlate with the NO reduction reactivity of the chars.

Acknowledgements

This project is funded by the Sino-Danish Centre for Education and Research and Technical University of Denmark. In addition, the Academy of Finland financed project (289666) – fate of fuel bound nitrogen in biomass gasification – is acknowledged.

References

(1) Glarborg, P.; Miller, J. A.; Ruscic, B.; Klippenstein, S. J. *Prog. Energy Combust. Sci.* **2018**, *67*, 31–68.

(2) Hupa, M.; Karlström, O.; Vainio, E. *Proc. Combust. Inst.* **2017**, *36* (1), 113–134.

(3) Johnsson, J. E. *Fuel* **1994**, *73* (9), 1398–1415.

(4) Glarborg, P.; Jensen, A. D.; Johnsson, J. E. *Prog. Energy Combust. Sci. 29* **2003**, *29*, 89–113.

(5) Jensen, L.; Jannerup, H.; Glarborg, P.; Jensen, A.; Dam-Johansen, K. *Proc. Combust. Inst.* **2000**, *28*, 2271–2278.

(6) Zhao, K.; Glarborg, P.; Jensen, A. D. *Energy & Fuels* **2013**, *27*, 7817–7826.

(7) Chambrion, P.; Kyotani, T.; Tomita, A. *Energy & Fuels* **1998**, *12* (2), 416–421.

(8) Karlström, O.; Perander, M.; DeMartini, N.; Brink, A.; Hupa, M. *Fuel* **2017**, *190*, 274–280.

(9) De Soete, G. G. *Symp. Combust.* **1991**, *23* (1), 1257–1264.

(10) Ulusoy, B.; Wu, H.; Lin, W.; Karlström, O.; Li, S.; Song, W.; Glarborg, P.; Dam-Johansen, K. *Fuel* **2019**, *236* (August 2018), 297–305.

(11) Karlström, O.; Wu, H.; Glarborg, P. *Fuel* **2019**, *235* (August 2018), 1260–1265.

(12) Sørensen, C. O.; Johnsson, J. E.; Jensen, A. *Energy and Fuels* **2001**, *15* (6), 1359–1368.

(13) Thomas, K. M. *Fuel* **1997**, *76* (6), 457–473.

(14) Aarna, I.; Suuberg, E. M. *Fuel* **1997**, *76* (6), 475–491.

(15) Molina, A.; Eddings, E. G.; Pershing, D. W.; Sarofim, A. F. *Prog. Energy Combust. Sci.* **2000**, *26*, 507–531.

(16) Dong, L.; Gao, S.; Song, W.; Xu, G. *Fuel Process. Technol.* **2007**, *88* (7), 707–715.

(17) Zhong, B. J.; Tang, H. *Combust. Flame* **2007**, *149* (1–2), 234–243.

(18) Wu, X.; Song, Q.; Zhao, H.; Zhang, Z.; Zhang, L.; Yao, Q. *Fuel* **2013**, *113*, 553–559.

(19) Zhao, Z.; Li, W.; Li, B. *Fuel* **2002**, *81* (11–12), 1559–1564.

(20) Commandré, J.-M.; Stanmore, B. R.; Salvador, S. *Combust. Flame* **2002**, *128*, 211–216.

(21) Konttinen, J.; Kallio, S.; Hupa, M.; Winter, F. *Fuel* **2013**, *108*, 238–246.

(22) Molina, A.; Murphy, J. J.; Winter, F.; Haynes, B. S.; Blevins, L. G.; Shaddix, C. R. *Combust. Flame* **2009**, *156* (3), 574–587.

(23) Aho, A.; DeMartini, N.; Pranovich, A.; Krogell, J.; Kumar, N.; Eränen, K.; Holmbom, B.; Salmi, T.; Hupa, M.; Murzin, D. Y. *Bioresour. Technol.* **2013**, *128*, 22–29.

(24) Zevenhoven, M.; Yrjas, P.; Skrifvars, B. J.; Hupa, M. *Energy and Fuels* **2012**, *26* (10), 6366–6386.

(25) Khazraie Shoulaifar, T.; Demartini, N.; Zevenhoven, M.; Verhoeff, F.; Kiel, J.; Hupa, M. *Energy and Fuels* **2013**, *27* (10), 5684–5690.

(26) Benson, S. A.; Holm, P. L. *Ind. Eng. Chem. Prod. Res. Dev. Chem. Prod. Res. Dev* **1985**, *2* (1), 145–149.

(27) Tchoffor, P. A.; Moradian, F.; Pettersson, A.; Davidsson, K. O.; Thunman, H. *Energy and Fuels* **2016**, *30* (12), 10435–10442.

(28) Wu, S. L.; Iisa, K. *Energy & Fuels* **1998**, *12*, 457–463.

(29) Levy, J. M.; Chan, L. K.; Sarofim, A. F.; Beér, J. M. *Symp. Combust.* **1981**, *18* (1), 111–120.

(30) Guo, F.; Hecker, W. C. *Symp. Combust.* **1996**, *26*, 2251–2257.

(31) Guo, F.; Hecker, W. C. *Symp. Combust.* **1998**, *27* (2), 3085–3092.

(32) Schönenbeck, C.; Gadiou, R.; Schwartz, D. *Fuel* **2004**, *83* (4–5), 443–450.

(33) Garijo, E. G.; Jensen, A. D.; Glarborg, P. *Energy & Fuels* **2003**, *17*, 1429–1436.

(34) Garijo, E. G.; Jensen, A. D.; Glarborg, P. *Combust. Flame* **2004**, *136* (1–2), 249–253.

(35) Kapteijn, F.; Moulijn, J. A.; Matzner, S.; Boehm, H. **1999**, *37*, 1143–1150.

(36) Ninomiya, Y.; Yokoi, K.; Arai, N.; Hasatani, M. *Int. Chem. Eng.* **1989**, *29* (3), 512–516.

(37) Winter, F.; Löffler, G.; Wartha, C.; Hofbauer, H.; Preto, F.; Anthony, E. J. *Can. J. Chem. Eng.* **1999**, *77*, 275–283.

(38) Molina, A.; Sarofim, A. F.; Ren, W.; Lu, J.; Yue, G.; Beér, J. M.; Haynes, B. S. *Combust. Sci. Technol.* **2002**, *174* (11–12), 43–71.

(39) Feng, B.; Liu, H.; Yuan, J.; Lin, Z.; Liu, D.; Leckner, B. *Energy & Fuels* **1996**, No. 10, 203–208.

(40) López, D.; Calo, J. *Fuel* **2007**, *86*, 1900–1907.

(41) Johnsson, J. E.; Jensen, A. *Proc. Combust. Inst.* **2000**, *28*, 2353–2359.

(42) Karlström, O.; Brink, A.; Hupa, M. *Energy & Fuels* **2013**, *27*, 1410–1418.

(43) Hayhurst, A. N.; Lawrence, A. D. *Prog. Energy Combust. Sci.* **1992**, *18*, 529–552.

(44) Dong, L.; Gao, S.; Song, W.; Xu, G. *Fuel Process. Technol.* **2007**, *88* (7), 707–715.

(45) Guerrero, M.; Millera, Á.; Alzueta, M. U.; Bilbao, R. *Energy & Fuels* **2011**, *25*, 1024–1033.

(46) Wu, X. Y.; Song, Q.; Zhao, H. B.; Zhang, Z. H.; Yao, Q. *Environ. Sci. Technol.* **2014**, *48* (7), 4184–4190.

(47) Pevida, C.; Arenillas, A.; Rubiera, F.; Pis, J. J. *Fuel* **2005**, *84* (17), 2275–2279.

(48) Chambrion, P.; Orikasa, H.; Suzuki, T.; Kyotani, T.; Tomita, A. *Fuel* **1997**, *76* (6), 493–498.

(49) Pels, J. R.; Kapteijn, F.; Moulijn, J. A.; Zhu, Q.; Thomas, K. M. *Carbon N. Y.* **1995**, *33* (11), 1641–1653.

(50) Xu, J.; Sun, R.; Ismail, T. M.; Sun, S.; Wang, Z. *Energy and Fuels* **2017**, *31* (12), 13406–13415.

(51) Phiri, Z.; Everson, R. C.; Neomagus, H. W. J. P.; Wood, B. J. *J. Anal. Appl. Pyrolysis* **2017**, *125* (July 2016), 127–135.

(52) Stańczyk, K. *Energy and Fuels* **1999**, *13* (1), 82–87.

(53) Stańczyk, K. *Energy and Fuels* **2004**, *18* (2), 405–409.

(54) Darvell, L. I.; Brindley, C.; Baxter, X. C.; Jones, J. M.; Williams, A. *Energy and Fuels*

2012, *26* (11), 6482–6491.

(55) Liu, X.; Luo, Z.; Yu, C. *Fuel* **2019**, *242* (September 2018), 389–397.

(56) Wu, H.; Castro, M.; Jensen, P. A.; Frandsen, F. J.; Glarborg, P.; Dam-Johansen, K.; Røkke, M.; Lundtorp, K. *Energy and Fuels* **2011**, *25* (7), 2874–2886.

(57) Chambrion, P.; Kyotani, T.; Tomita, A. *Symp. Combust.* **1998**, *27*, 3053–3059.